NASA TECHNICAL NOTE

NASA TN D-4533

c. 1

NASA TN D-4533

ELECTRICAL PERFORMANCE OF A RHENIUM-NIOBIUM CYLINDRICAL THERMIONIC CONVERTER

by Richard M. Williams and William J. Bifano

Lewis Research Center
Cleveland, Ohio

NATIONAL AERONAUTICS AND SPACE ADMINISTRATION • WASHINGTON, D. C. • APRIL 1968

NASA TN D-4533

ELECTRICAL PERFORMANCE OF A RHENIUM-NIOBIUM CYLINDRICAL THERMIONIC CONVERTER

By Richard M. Williams and William J. Bifano

Lewis Research Center
Cleveland, Ohio

NATIONAL AERONAUTICS AND SPACE ADMINISTRATION

For sale by the Clearinghouse for Federal Scientific and Technical Information
Springfield, Virginia 22151 – CFSTI price $3.00

ABSTRACT

The electrical performance of a cylindrical rhenium-niobium thermionic converter was measured by a pulse technique for the following temperatures: emitter, 1873° to 2073° K; collector, 850° to 1050° K; and cesium reservoir, 590° to 670° K. The peak output power densities at 1873°, 1973°, and 2073° K were 7.0, 9.4, and 11.4 W/cm^2 at 0.4, 0.5, and 0.6 V, respectively. The corresponding collector temperatures were about 900°, 940°, and 950° K, and the cesium reservoir temperatures were 595°, 606°, and 611° K. The Rasor-Warner correlation was used to estimate a 5.0±0.1 V work function for the vapor-deposited rhenium emitter.

ELECTRICAL PERFORMANCE OF A RHENIUM-NIOBIUM CYLINDRICAL THERMIONIC CONVERTER

by Richard M. Williams and William J. Bifano

Lewis Research Center

SUMMARY

The electrical performance of a cylindrical thermionic converter is described. The electrically heated converter had a vapor-deposited rhenium emitter electrode and a niobium collector electrode. Performance was measured over an emitter temperature range of 1873° to 2073° K, a collector temperature range of 850° to 1050° K, and a cesium reservoir temperature range of 590° to 670° K. The dependence of the converter power density on changes in the cesium reservoir and electrode temperatures is shown. A determination of the emitter work function is included.

The results indicate that the converter maximum power density increased from 7.0 to 11.4 watts per square centimeter as the emitter temperature was raised from 1873° to 2073° K. For this range of emitter temperatures, the power density maximized over the following limited range of the other system variables: collector temperatures, 900° to 950° K; cesium reservoir temperature, 595° to 613° K; and electrode voltage, 0.4 to 0.6 volt.

INTRODUCTION

Thermionic conversion of heat to electrical power is a promising technique for generating power in space. Thermionic converters may be coupled with solar, radioisotope, or nuclear-reactor heat sources, with the reactor in-core system being of particular interest for high-power missions.

Cylindrical converters would be used for the in-core application with the emitting electrode serving as the clad for the reactor fuel. At the present time, only a few performance data are available for cylindrical converters operating over a range of electrode temperature. One such performance investigation was conducted with two cylindrical converters, both having a tungsten emitter, one having a niobium collector, and the other having a molybdenum collector. The performance was reported in 1963 (ref. 1).

For the past several years, research programs in thermionic conversion have been

directed toward improving performance by improving electrode materials. Improved electrode materials are now available and it is desirable to evaluate these materials in converters having the cylindrical geometry required by the reactor in-core concept.

Reported herein is the performance of a cylindrical thermionic converter having a rhenium emitter and a niobium collector. The converter was electrically heated, cesiated, and had an emitter electrode area of 15.2 square centimeters. The converter performance at peak output power is emphasized.

Output power was determined over the following ranges of electrode and cesium-reservoir temperatures: emitter temperature, 1873° to 2073° K; collector temperature, 850° to 1050° K; and cesium-reservoir temperature, 590° to 623° K. The bare work function of the vapor-deposited rhenium emitter was also determined.

CONVERTER DESIGN AND THERMOCOUPLE INSTRUMENTATION

The converter was designed to the specifications of Lewis Research Center personnel and was constructed by Thermo Electron Engineering Corporation. A cross-sectional drawing of the converter is shown in figure 1. It is electrically heated, cylindrical, and cesiated, and it was operated in a vacuum enclosure. Emitter and collector heaters are incorporated to allow operation over a wide range of electrode temperatures.

The rhenium emitter is heated by electron bombardment from a helical tungsten filament positioned in the emitter cavity as shown in figure 1. The emitter surface is rhe-

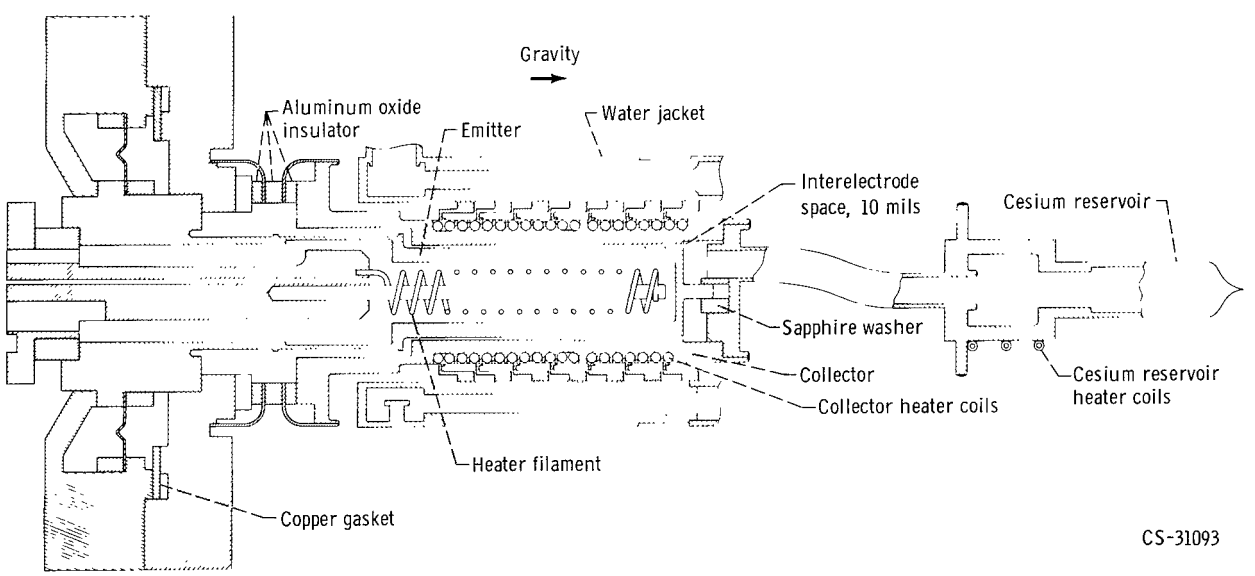

Figure 1. - Layout drawing of cylindrical thermionic converter.

nium, which was vapor deposited on a tantalum substrate. The rhenium thickness was nominally 0.38 millimeter (15 mils), and the total emitter wall thickness was 2.03 millimeters (80 mils). The cup-shaped emitter is 1.27 centimeters (0.502 in.) in diameter with an axial length of 3.81 centimeters (1.50 in.), resulting in a total active emitter area of 15.2 square centimeters. The emitter assembly is demountable and has the usual provisions for stress relief.

A niobium collector assembly is positioned coaxially with the emitter and has a wall thickness of 3.56 millimeters (140 mils). The interelectrode spacing is 0.254 millimeter (0.010 in.) at room temperature. This spacing is maintained by machined shoulders at the top of the emitter structure providing both lateral and axial positioning. A rhenium positioning pin is also included on the lower end of the emitter and inserted into a sapphire insulator brazed to the collector structure.

An insulating ceramic-to-metal seal was electron-beam welded to the top of the collector assembly to provide electrical isolation from the emitter structure. Two parallel helical grooves were cut into the collector outer diameter into which were placed two tantalum sheathed resistive heater elements. These heaters were electrically connected in parallel. Outboard of the collector and its heater are seven niobium fins which act as heat chokes between the collector and the water-cooled heat exchanger.

Eighteen thermocouples were installed in the converter. Three axial wells are provided in the emitter wall into which thermocouples are inserted for measuring top, middle, and bottom emitter temperatures. Thermocouples are positioned at points 3.8, 19.7, and 36.2 millimeters (0.150, 0.775, and 1.425 in.) from the active emitter top. These (W - 5Re/W - 25Re) emitter thermocouples are sheathed with tantalum and have a 1.02-millimeter (40-mils) diameter. A second set of emitter thermocouple wells were provided as spares. Three Chromel-Alumel (C-A) thermocouples are inserted radially into the collector wall to measure the top, middle, and bottom collector temperatures. These thermocouples are located at the same axial position as the corresponding emitter thermocouples.

Three C-A thermocouples are attached to the cesium reservoir. Two are used to locate the coldest point in the reservoir. The third is used to control the reservoir temperature by means of a temperature controller which regulates the cesium heater power.

Additional thermocouples are added to monitor the temperatures of various seals and assemblies.

Diode Processing

Following the vapor deposition of rhenium onto the machined tantalum substrate, the emitter surface was ground to dimension. A 100-grit diamond wheel was initially employed in the grinding operation. Final grinding, resulting in a 10 to 12 rms finish, was

accomplished with a 45-grit alumina wheel. The electrode was neither electropolished nor electroetched. The emitter was then thermally annealed at a brightness temperature of 2200° K (estimated 2400° K true) for a period of 10 minutes in a vacuum of 2×10^{-6} torr (3×10^{-4} N/m^2).

After annealing, photomicrographs (×150) were taken of the emitter surface. A representative photograph is shown in figure 2. The area shown is approximately 0.64 by

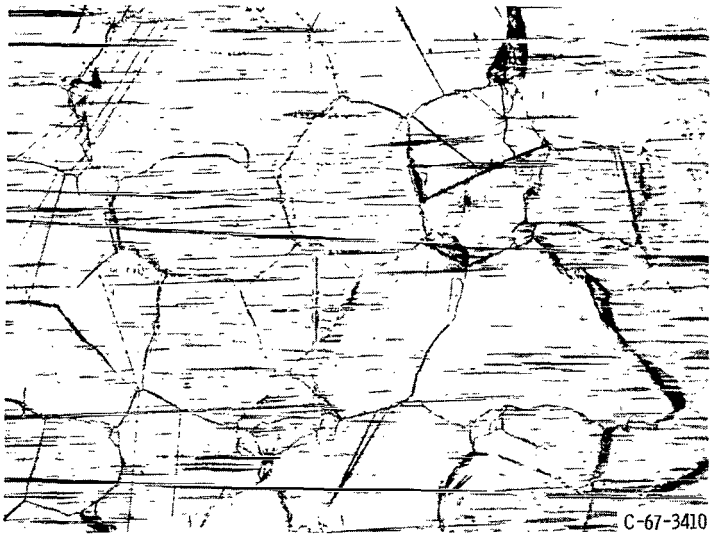

Figure 2. - Photomicrograph of rhenium emitter surface showing circumferential grinding marks.

0.48 millimeter. The circumferential grinding marks are prominent, as are the irregular shapes of the rhenium grains.

The collector electrode cavity was stone honed and polished to a 10 to 15 rms finish with emery paper. No photographs were taken of this surface.

After joining, the emitter-collector assembly underwent a 35-hour outgassing. The assembly was mounted in a bell jar which was maintained at a pressure of 6×10^{-6} torr (8×10^{-4} N/m^2), while the interelectrode cavity was evacuated with a standard titanium-ion pump connected to the cesium reservoir tubulation. The assembly was heated using both the emitter electron-bombardment heater and the collector and cesium-reservoir heaters. During this operation, no coolant was passed through the heat exchanger. The temperatures of the assemblies were gradually increased during the bakeout time while maintaining the interelectrode pressure below 7×10^{-7} torr (9×10^{-5} N/m^2) as measured at the pump.

The bakeout was completed when the following assembly temperatures were reached with a pump pressure of 4×10^{-7} torr (5×10^{-5} N/m^2): cesium-reservoir temperature,

760° K; collector temperature, 1060° K; observed emitter temperature, 1775° K. The emitter temperature was observed at one of the two hohlraums provided. Because of the hohlraum position, it is estimated that this temperature was at least 300° C below the maximum emitter temperature.

After cooling the assembly, liquid cesium was double distilled into the cesium reservoir using a tubulation which had previously been attached to the converter-reservoir - ion-pump tubulation. When the cesium vial was crushed a pump pressure rise from 5×10^{-8} to 2×10^{-5} torr was observed. The cesium was initially distilled at 200° C for 1/2 hour into a cooled intermediate reservoir. From this intermediate reservoir, a second distillation process transferred the liquid cesium to the converter reservoir. Following the second distillation, the copper tubulation was pinched off, sealing the converter.

Experimental Circuit and Procedures

The converter was connected into the load circuit shown in figure 3. The oscilloscope was operated in the XY mode to record the converter current-voltage output. The converter electrode voltage probes were connected to the horizontal channel of the oscilloscope; the voltage probes from the diode current shunt were connected to the other oscilloscope channel.

The unique feature of this circuit is the transformer coupling of a pulse circuit.

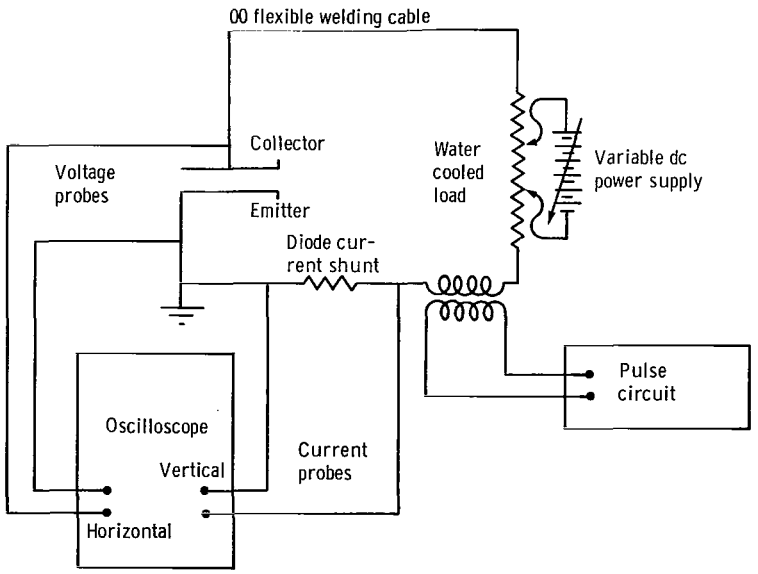

Figure 3. - Schematic diagram of data-taking circuit.

This pulse circuit, designed by Lewis personnel (private communication from M. Tiefermann), perturbs the converter voltage in the main circuit by introducing 1 cycle of 60-hertz sinusoidal voltage to this circuit. This voltage pulse is adjustable from 0 to 5 volts peak-to-peak. The advantage of this technique is that the characteristic current-voltage response of the converter can be instantaneously recorded with the oscilloscope while the converter temperature levels are relatively unaffected by the slight change in heat transfer.

A typical data point is described in appendix A; a detailed description of the auxiliary equipment required to support the testing of the converter is included in appendix B.

Between tests, the converter was stored in a vacuum below 10^{-6} torr ($\sim 10^{-4}$ N/m^2), maintained by a vacuum-ion pump. The converter was exposed to the atmosphere only when it was necessary to make repairs.

Prior to operation, the converter was heated slowly to minimize thermal stresses. During heating, the cesium reservoir temperature was maintained as the coldest spot in the region exposed to cesium vapor. The initial data point each day was a repeat point. At a set reservoir temperature, predetermined collector and filament bombardment power supply settings were repeated with the converter at open circuit. After temperature stabilization, the assembly temperatures and the open circuit voltage were compared with previous repeat runs. Periodically, current-voltage characteristic curves were repeated and compared. In this manner, any diode performance changes or instrumentation problems could be quickly detected. After all the selected data had been recorded, the diode was cooled slowly to minimize thermal stresses.

The following technique was used to determine the electrode and cesium-reservoir temperatures required to obtain maximum electrode power density. The current-voltage characteristics of the converter were recorded at 14 possible combinations of the electrode temperatures: three emitter temperatures (i.e., 1873°, 1973°, and 2073° K) and five collector temperatures (i.e., 850°, 900°, 950°, 1000°, and 1050° K). (The 850° K collector temperature at 1973° K emitter temperature was omitted.) At each of these 14 conditions, the cesium-reservoir temperature was changed in increments of 5° K over a range which included the maximum power-density condition. Pulsed current-voltage responses of the converter were recorded at each point. Thus, for any selected electrode temperature combination, the condition yielding the highest power density could easily be determined.

Initially, the effective electrode temperatures (i.e., emitter and collector temperatures) were determined as follows. For a given case, the three electrode temperatures were plotted as functions of their respective thermocouple locations. A smooth curve was then drawn through the points and the area under the curve accurately measured with a planimeter. This area, representing

$$\int_0^{l} T(x)dx$$

(where x is the axial distance along the electrode) was then divided by the electrode length l to determine the effective electrode temperature. Because of the large number of runs involved, an alternate technique was eventually formulated which permitted the use of a digital computor. Since the electrode end point thermocouples were located a short distance from the actual physical ends of the electrode, a linear extrapolation was used to extend the temperature curve. These extrapolated end-point temperatures and the center-electrode temperature were then used to compute the effective electrode temperature using Simpson's rule. Applications of this technique to over 100 cases initially evaluated using the planimeter yielded deviations in effective electrode temperature of less than $\pm 2^{o}$ K. This computor technique was then used for the remainder of the test program to determine effective electrode temperature.

PRECISION OF DATA

In table I, the accuracy of each important sensor and measuring instrument is tabulated. An estimate of the maximum error of each thermocouple reading is included. The instrument error given indicates the reproducibility of each thermocouple reading. The maximum uncertainty is the sum of the reading instrument error and the thermocouple error.

The W - 5Re/W - 25Re emitter thermocouples were individually calibrated by Thermo-Electron Corporation. The absolute error of this calibration at 2000^{o} K is estimated to be $\pm 30^{o}$ K. The instrument error of 0.7^{o} K is insignificant at the emitter temperatures of interest.

An additional uncertainty in the emitter temperature is due to the electron cooling of the emitter. If the average current occurring during a voltage sweep is higher than that of the steady-state point at which the temperatures are recorded, the increased electron cooling decreases the emitter temperature. The temperature change varies with each sweep data point. It is estimated that the average temperature at maximum power is 10^{o} K lower than the initial temperature.

Also included in table I is an estimate of the precision of the electrical measurement of the converter output. The reading error is the error in recording the current and voltage from the oscilloscope photographs (appendix A). An absolute instrument error of ± 3.0 percent is quoted by the oscilloscope manufacturer. The instrument error is greater than the reading error.

In figure 4, the calculated uncertainty in the power density is plotted as a function of

TABLE I. - PRECISION OF DATA

(a) Temperatures

Location	Thermocouple		Relative or instrument error	Estimated total error
	Type	Error		
Emitter	W 5 Re - W 25 Re	$\pm 30^{\circ}$ K at 2000° K	Digital voltmeter, ± 0.01 mV and $\pm 0.67^{\circ}$ K	$\pm 40^{\circ}$ K at 2000° K
Collector	K Chromel-Alumel	± 0.75 percent	Strip chart recorder, self referenced, $\pm 2.5^{\circ}$ K	$\pm 8^{\circ}$ K at 1000° K
Cesium reservoir	K Chromel-Alumel	± 0.75 percent	Digital voltmeter, ± 0.01 mV; reference oven, $\pm 1^{\circ}$ F ($\pm 0.55^{\circ}$ K)	$\pm 3.0^{\circ}$ K at 628° K

(b) Electrical performance

Item	Reading error	Instrument error, percent	*Maximum uncertainty*
Diode voltage	± 0.01 V	± 3.0	0.04 V at 1.00 V
Diode current density	± 0.13 A/cm^2	± 3.0	0.73 A/cm^2 at 20 A/cm^2
Power density	----------	----	0.95 W/cm^2 at 11.4 W/cm^2

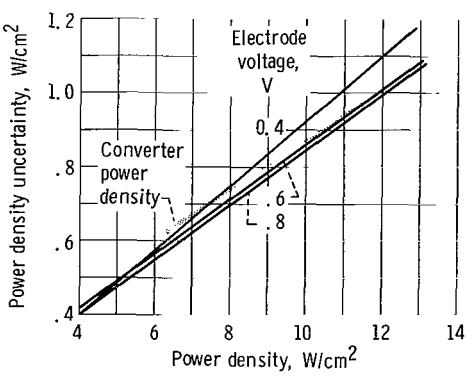

Figure 4. - Uncertainty of power density measurements at three electrode voltages.

the total power density for a number of fixed electrode voltages. The converter power-density data shown in the cross-hatched region illustrates the range of voltage over which the maximum power density was achieved. The calculations assume an oscilloscope instrument error of 3.0 percent for both the current and voltage. Reading errors are ±2.0 amperes or ±0.13 ampere per square centimeter (A/cm^2) and ±0.01 volt. As a result of these errors, at a power density of 6.0 watts per square centimeter (W/cm^2) at 0.40 volt the uncertainty is 0.49 W/cm^2. At a power density of 11.0 W/cm^2 at 0.80 volt the uncertainty is ±0.92 W/cm^2. The resulting uncertainty is nearly 8 percent of the power density.

RESULTS AND DISCUSSION

Dependence of Power Density on Temperature

The dependence of the converter power density on the cesium-reservoir temperature is shown in figure 5. This figure is in three sections, one for each emitter temperature. Each section illustrates the changes of power density with cesium reservoir temperature for each of the five collector temperatures. At each combination of electrode and cesium reservoir temperature, the highest achievable power density is computed from the current-voltage curve as described in appendix A.

When the emitter temperature was raised from 1873° to 2073° K, the peak power attainable increased from 7.0±0.65 to 11.4±0.95 W/cm^2. At fixed collector temperature, the reservoir temperature required for peak power increased with increasing emitter temperature. Also, at fixed emitter temperature, as the collector temperature was raised, peak power was obtained at steadily increasing reservoir temperatures.

Figure 6 is a cross plot of the data of figure 5. The abscissa is the emitter temperature with the cesium reservoir temperature and electrode voltage selected to provide maximum power density. For all collector temperatures, the power density increases nearly linearly with the emitter temperature. For example, at a collector temperature of 900° K, the power density increases from about 7 to 11 W/cm^2 as the emitter temperature is raised from 1873° to 2073° K.

In figure 7 power density is plotted against collector temperature with emitter temperature as a parameter. Notice that the collector temperature required for peak power increases as the emitter temperature is raised. If the cesium reservoir temperature and the electrode voltage were fixed at the maximum power point, changes in the collector temperature would cause greater changes in the power density than shown in figure 7. Operating the converter at a collector temperature of 1050° K, the highest heat-rejection temperature studied, resulted in a significant reduction in the power density. However,

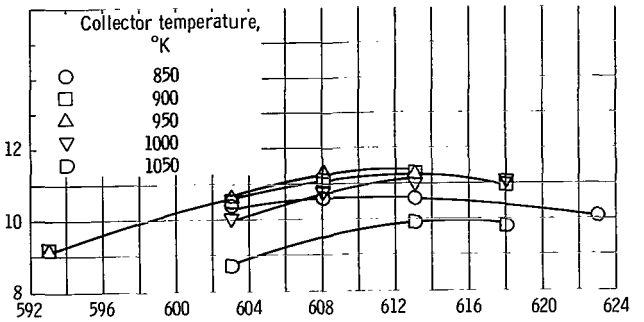

(a) Emitter temperature, 2073° K.

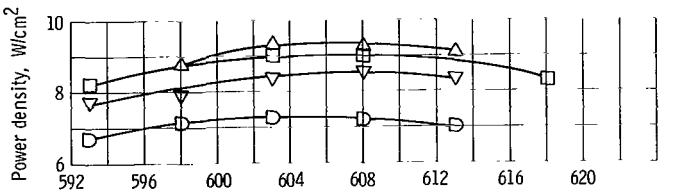

(b) Emitter temperature, 1973° K.

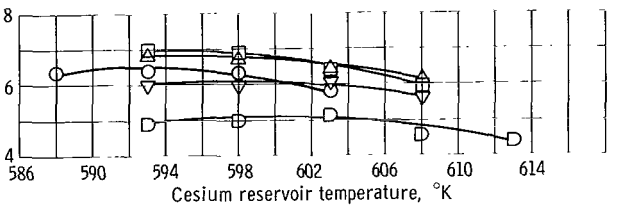

(c) Emitter temperature, 1873° K.

Figure 5. - Converter performance at output voltage producing highest output power.

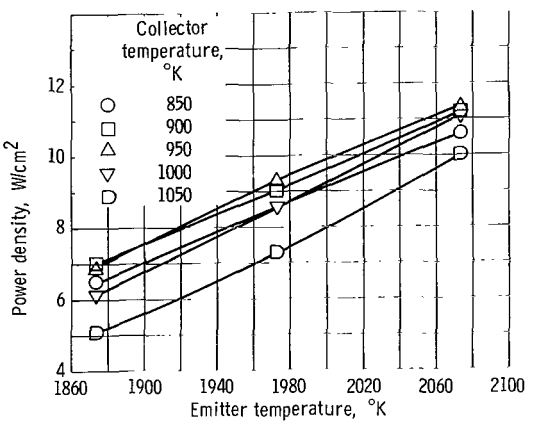

Figure 6. - Converter performance at voltage and cesium reservoir temperature producing peak power.

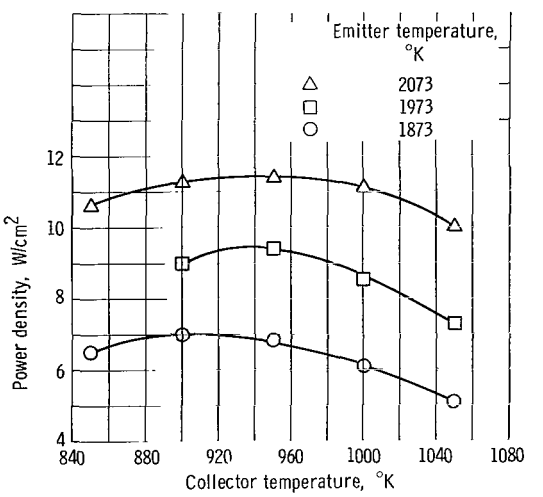

Figure 7. - Variation in converter performance with collector temperature at constant emitter temperature; voltage and reservoir temperature selected for peak power.

it would be necessary to study an application in detail in order to determine whether operating at this collector temperature would penalize or improve the overall performance of a proposed power system.

The effect of cesium reservoir temperature on the voltage near peak power is shown in figure 8. The collector temperature is 950° K and, as can be seen in figure 7, is near the maximum power condition. The dashed line indicates the voltage at which the maximum power was achieved for each emitter temperature at this fixed collector temperature. The voltage ranges from 0.43 to 0.65 volt as the emitter temperature is raised from 1873° to 2073° K. The higher voltage implies both lower joule losses in the power leads and a possible advantage in power conditioning.

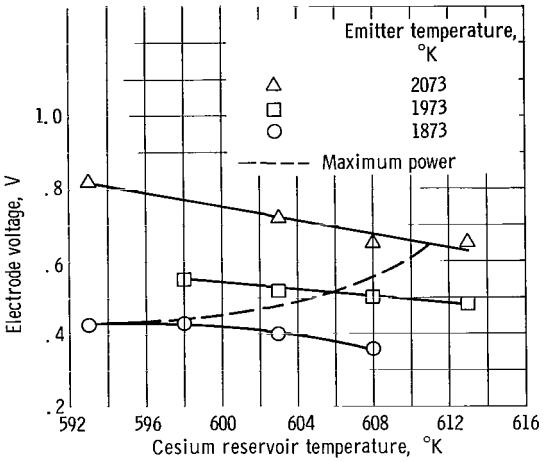

Figure 8. - Variation in voltage output at peak power due to changes in reservoir temperature; collector temperature, maintained at 950° K.

Emitter Work Function Determination

Electron saturation current measurements were made over an emitter temperature range of 1600° to 2100° K under ion-rich conditions (ion-rich conditions exist when the number of ions present exceed that required for space charge neutralization). For cases in which the saturation current was well defined (i.e., in which a change in electrode voltage resulted in no change in current), the emitter cesiated work function φ in volts was calculated using the Richardson-Dushman equation:

$$\varphi = \frac{kT_E}{e} \ln \frac{120\ T_{E2}}{J_s} \tag{1}$$

where

T_E average emitter temperature, ^oK

k Boltzmann's constant, 1.3805×10^{-23} J/^oK

e electron charge, 1.602×10^{-19} C

J_s electron current density, A/cm^2

The integrated mean emitter temperature

$$\frac{1}{L}\int_0^l T(x)dx$$

was used as the "effective" emitter temperature. Temperature variations along the surface of the emitter (axially) between about 50^o and 200^o K were observed in obtaining saturation current. A more precise technique requires recognition of the nonlinear current-temperature relation; however, the simpler averaging technique was considered adequate for this study.

The cesiated work function obtained from equation (1) was plotted against the ratio of emitter temperature to cesium reservoir temperature T_E/T_{cs} (fig. 9). A comparison of the resultant curve with theoretically determined curves (ref. 2) was then made to determine the work function of the bare-rhenium surface. As shown in figure 9, the data

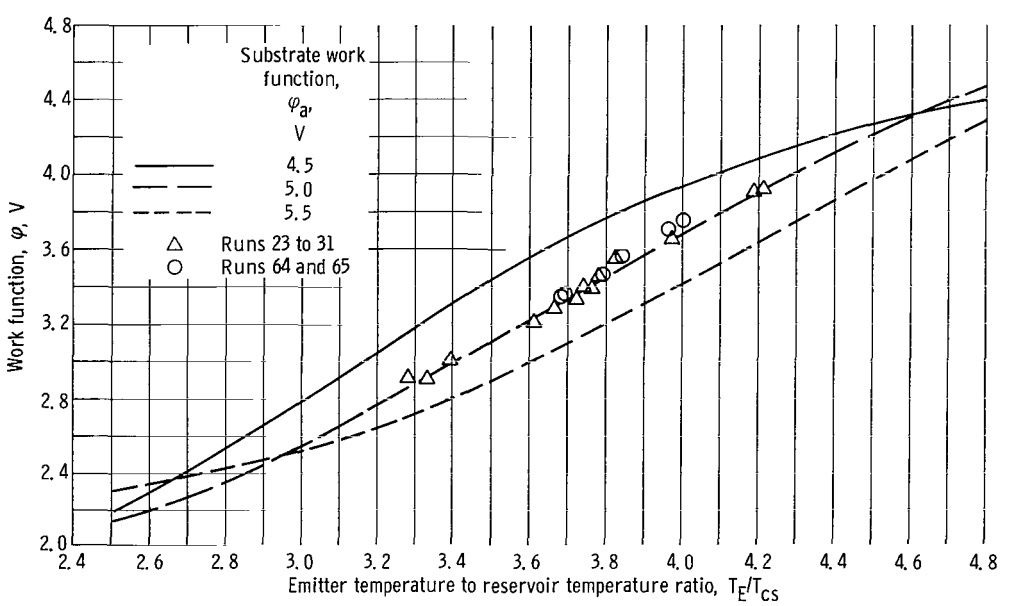

Figure 9. - Cesiated emitter work function plotted against emitter to cesium reservoir temperature ratio.

TABLE II. - DATA USED TO DETERMINE EMITTER BARE WORK FUNCTION

Run	Current density, A/cm^2	Mean emitter temperature, ^oK	Cesium reservoir temperature, ^oK	Ratio of emitter temperature to cesium-reservoir temperature, T_E/T_{Cs}	Work function, V
28-2	0.296	1864	498	3.74	3.39
28-4	.493	1854	508	3.66	3.28
28-5	.526	1667	508	3.28	2.91
28-6	.394	1690	498	3.39	3.00
28-7	.401	1641	493	3.33	2.90
29-2	.415	1826	498	3.66	3.27
29-3	.194	1832	488	3.76	3.39
29-4	.303	1836	493	3.72	3.33
29-5	.210	1863	493	3.78	3.45
29-7	.256	1984	500	3.97	3.65
29-8	.194	2084	498	4.19	3.90
29-15	.276	1765	489	3.61	3.20
30-4	.194	1914	500	3.82	3.55
30-5	.118	2051	487	4.21	3.92
64-2	.282	1839	498	3.68	3.34
65-7	.330	1856	503	3.69	3.36
65-8	.202	1890	493	3.79	3.46
65-9	.263	1935	503	3.84	3.56
65-10	.210	1994	503	3.96	3.70
65-11	.204	2015	504	4.00	3.75

points correspond to a bare work function of 5.0±0.1 volts. This value may be high due to the aforementioned method of averaging temperature; however, it is in agreement with previously measured values of the work function of polycrystalline rhenium which range from 4.7 to 5.1 volts (refs. 3 and 4, respectively). The data used to determine bare-emitter work function presented in table II were reproducible over an 8-month period, which represents over 1000 hours of diode operation.

SUMMARY OF RESULTS

The parametric investigation of the performance of an electrically-heated cesiated, cylindrical rhenium-niobium thermionic converter using pulse data acquisition techniques produced the following results:

1. For the conditions studied, the peak power changes with emitter temperature as follows:

Emitter temperature, ^{o}K	Maximum achievable power density, W/cm^2
1873	7.0±0.65
1973	9.4±0.80
2073	11.4±0.95

2. For the range of emitter temperatures considered, the collector and cesium reservoir temperatures and the electrode voltage at peak power change over a narrow range. The values of these three parameters increase with increasing emitter temperature as follows:

Parameter	Emitter temperature, ^{o}K		
	1873	1973	2073
Collector temperature, ^{o}K	900	940	950
Cesium reservoir temperature, ^{o}K	595	606	611
Electrode voltage, V	0.4	0.5	0.6

3. The cesiated work function of the emitter electrode, mechanically polished, vapor-deposited rhenium, was determined from saturation current measurements obtained over a broad range of emitter and cesium reservoir temperatures. From the correlation of reference 2, the bare work function was estimated to be 5.0±0.1 volts.

Lewis Research Center,
National Aeronautics and Space Administration,
Cleveland, Ohio, September 20, 1967,
120-27-05-01-22.

APPENDIX A

TYPICAL DATA POINT

Description of Current-Voltage Trace

Figure 10(a) is a typical current-voltage oscilloscope photograph. The total converter current (i.e., the product of current density and emitter area) is displayed vertically as a function of the converter electrode voltage. The steady-state point is indicated by a spot surrounded by a halo. As read by the digital voltmeter, the steady-state point is at 0.640 volt and 172 amperes, which closely agrees with the estimated center of the spot shown in the photograph. (For this photograph, the emitter temperature is 1973° K, the collector temperature is 1000° K, and the cesium reservoir temperature is 608° K.)

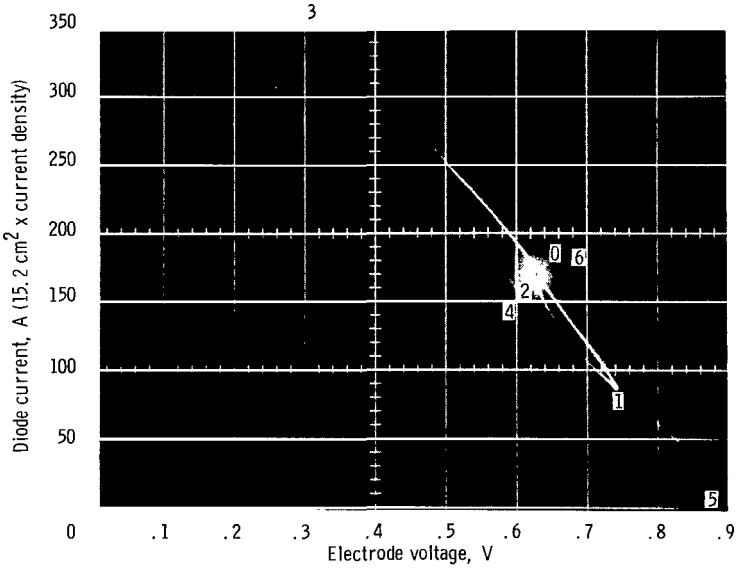

(a) Typical current-voltage trace oscilloscope photograph.

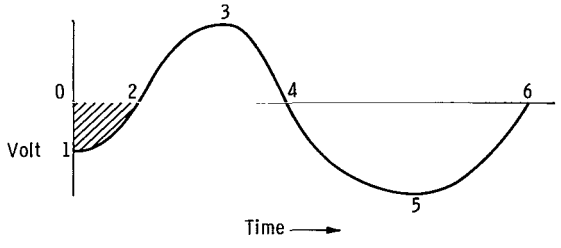

(b) Typical voltage-wave form.

Figure 10. - Characteristics of a typical data point.

For each data point a voltage pulse of the form shown in figure 10(b) is impressed on the converter. Because of circuitry problems, an extraneous portion of the waveform, shown by cross-hatching, is included. This portion is not included in the data analysis. Starting at the steady-state point shown in figure 10, the current is varied continuously, as indicated, from point 0 to point 6. Hysteresis of this trace is noticeable (i.e., the current of the return trace is lower than the initial sweep for each electrode voltage). This hysteresis could be the result of a number of causes.

For example, hysteresis could be a result of a phase shift between the vertical and horizontal amplifier channels of the oscilloscope. However, input signals in the frequency range from 60 to 1000 hertz were simultaneously applied to both oscilloscope channels, and no hysteresis was detected.

Hysteresis might also be a result of phase shift in the data acquisition circuit and its associated probes. A dummy load, namely, a silicon diode, was substituted for the thermionic converter in the data acquisition circuit, and current-voltage characteristics were taken and compared. No hysteresis was detected in this series of tests.

A change of emitter temperature associated with changes in emitter electron cooling might be a source of hysteresis. The temperature change associated with the decreased current of the lower trace was estimated in the following manner. For a cesium reservoir temperature of 608° K and a collector temperature of 1000° K, the current-voltage curve at the three emitter temperatures was used. (The 1973° K data were taken from fig. 10(a).) For three fixed electrode voltages, the total current was plotted against the emitter temperature and is shown in figure 11. All data were taken from the upper trace of the oscilloscope readings. The current read from the lower trace of figure 10(a) for each voltage was plotted as a dashed line. The associated temperature change for each voltage can be observed.

A maximum temperature difference of about 30° K is indicated between the upper and lower current-voltage curves at 0.6 volt which is near the steady-state voltage of 0.64 volt. When it is assumed (1) that the inner wall of the emitter is held at constant temperature during the voltage pulse and (2) that the emitter responds instantaneously to changes in electron cooling, calculations indicate that a temperature decrease of 10° K would be expected when the current increases by 200 amperes. The 30° K temperature change indicated previously is reasonable because the inner-wall temperature would be expected to drop. Therefore, the hysteresis can be attributed to electron cooling of the emitter.

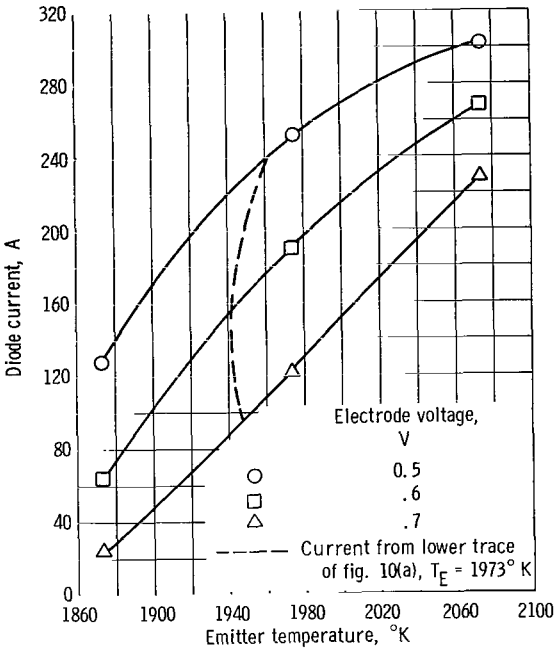

Figure 11. - Variations in converter current due to changes in emitter temperature; fixed collector and cesium-reservoir temperatures.

Description of Data Reduction Techniques

The current densities employed in this report are taken from the higher current trace of the characteristic current-voltage curves. All temperature measurements were made at the steady-state point, which is on the upper trace (fig. 10(a)). It was sometimes necessary to correct the sweep point current and voltage, which was indicated on the photograph, to the values read on the digital voltmeter.

Specifically, the maximum power density was computed in the following manner from the current-voltage characteristics shown in figure 10(a): The sweep electrode voltage readings observed on the photograph were corrected by +0.01 volt, which is the difference between the steady-state electrode voltage observed on the photograph and the

TABLE III. - READINGS TAKEN

FROM FIGURE 10(a)

Electrode voltage, V	Corrected electrode voltage, V	Current, A	Power, W	Power density, W/cm^2
0.42	0.43	300	129.0	8.5
.44	.45	288	129.6	8.5
.46	.47	278	130.4	8.6
.48	.49	263	128.9	8.5
.50	.51	252	128.5	8.4

voltage read by the digital voltmeter. The converter current is read from the photograph to within ±2 amperes (0.13 A/cm^2) at 0.02-volt increments near the maximum output power point, and these data are recorded in table III. For this particular case (i.e., emitter temperature, 1973° K; collector temperature, 1000° K; and cesium reservoir temperature, 608° K), the power density maximized at 8.6 W/cm^2 and 0.47 volt.

APPENDIX B

TEST EQUIPMENT

Emitter Power Supply

The dc bombardment power supply operates on 208 volts, ac (three phase, four wire), fused at 30 amperes. This unit supplies both ac filament heating power and dc power for electron bombardment heating of the emitter electrode. The ac output of this supply is variable from 0 to 20 volts with a maximum current rating of 50 amperes; the dc output is variable from 0 to 1000 volts with a maximum current of 4.0 amperes.

A floating three-wire output from this power supply contains two ac lines and one positive biased dc line. The negative high voltage dc line is made common to one of the ac conductors. The ac lines are attached to the electron-bombardment filament and the positive dc line is attached to the emitter. With ac filament power only, heat is transferred from the filament to the emitter by thermal radiation. The addition of dc accelerating voltage then results in additional heat input due to electron bombardment of the emitter.

Direct-Current Bias Power Supply

A dc power supply was incorporated in the diode circuit (fig. 3) in order to bias the diode output voltage. This highly filtered, 0.01-percent ripple power supply had a voltage output range of 0 to 12 volts with a current limit of 1500 amperes dc. A water-cooled, copper tube, variable-resistance load was used to shunt a portion of the output in order to increase control sensitivity.

Precision Shunts

A series of high-current shunts was used to give approximately 50-millivolt output over the range of currents studied. These shunts were all within 0.04 percent of the specified resistance value and ranged from 0.01 to 0.0002 ohm. All the high-current components (i.e., converter, load transformer, and shunt) of the main circuit were joined by 00 flexible welding cable.

Oscilloscope

A dual beam oscilloscope was used in an X-Y mode to record on film the instantaneous current-voltage response of the converter. The oscilloscope has an operating range of 200 microvolts to 20 volts per centimeter and was accurate to within 3 percent of the panel reading. This accuracy was verified periodically and was found to be stable. The input RC is 1 megohm paralleled by 47 picofarads. The differential input rejection ratio is 100 at 0.2 volt per centimeter for a 1-kilohertz sine wave input signal. This ratio increases to 40 000 for the 0.1 millivolt per centimeter scale.

REFERENCES

1. Holland, J. W.: Performance and Energy-Transfer Measurements on Cylindrical Cesium Thermionic Converters. Rep. No. GA-4729, General Dynamics Corp., Nov. 13, 1963.

2. Rasor, Ned S.; and Warner, Charles: Correlation of Emission Processes for Adsorbed Alkali Films on Metal Surfaces. J. Appl. Phys., vol. 35, no. 9, Sept. 1964, pp. 2589-2600.

3. Kitrilakis, S. S.; and Weinstein, J. H.: Thermionic Emitter Materials Research Program. Rep. No. 27-64, Thermo Electron Eng. Corp., 1963. (Available from DDC as AD-425895.)

4. Weast, Robert C., ed.: Handbook of Chemistry and Physics. 40th ed., Chemical Rubber Publishing Co., 1957, p. 2378.

NASA-Langley, 1968 —— 3 E-3777

"The aeronautical and space activities of the United States shall be conducted so as to contribute . . . to the expansion of human knowledge of phenomena in the atmosphere and space. The Administration shall provide for the widest practicable and appropriate dissemination of information concerning its activities and the results thereof."

—NATIONAL AERONAUTICS AND SPACE ACT OF 1958

NASA SCIENTIFIC AND TECHNICAL PUBLICATIONS

TECHNICAL REPORTS: Scientific and technical information considered important, complete, and a lasting contribution to existing knowledge.

TECHNICAL NOTES: Information less broad in scope but nevertheless of importance as a contribution to existing knowledge.

TECHNICAL MEMORANDUMS: Information receiving limited distribution because of preliminary data, security classification, or other reasons.

CONTRACTOR REPORTS: Scientific and technical information generated under a NASA contract or grant and considered an important contribution to existing knowledge.

TECHNICAL TRANSLATIONS: Information published in a foreign language considered to merit NASA distribution in English.

SPECIAL PUBLICATIONS: Information derived from or of value to NASA activities. Publications include conference proceedings, monographs, data compilations, handbooks, sourcebooks, and special bibliographies.

TECHNOLOGY UTILIZATION PUBLICATIONS: Information on technology used by NASA that may be of particular interest in commercial and other non-aerospace applications. Publications include Tech Briefs, Technology Utilization Reports and Notes, and Technology Surveys.

Details on the availability of these publications may be obtained from:

SCIENTIFIC AND TECHNICAL INFORMATION DIVISION

NATIONAL AERONAUTICS AND SPACE ADMINISTRATION

Washington, D.C. 20546